Design of a non-flapping seagull-inspired composite morphing drone

Moises Brambila[1], Alex Rini[1], Jordan Eghdamzamiri[1], Hariet Yousefi[1], Joshua Herrera[1], Donovan Hanna[1], Caleb Black[1], Youssef Saad[1], Aramar Arias-Rodas[1]
and
Peter L. Bishay[2]
Department of Mechanical Engineering, California State University, Northridge

Many avian species are well equipped for dynamic flight with flexible morphing wings and tails that optimize aerodynamic performance across various environmental conditions. Imitating the shape-changing anatomical characteristics of birds can result in unmanned aerial vehicle (UAV) designs that outperform conventional fixed-wing UAVs in terms of flight performance. This rationale is the guiding principle behind the extensive research of morphing wing structures in the aerospace community. This work presents "CGull", a bio-inspired, non-flapping UAV with wing and tail morphing capabilities. CGull's target weight, size, and airfoil profiles are based on the characteristics of the Great Black-Backed Gull (GBBG). A mathematical model was first developed in MachUpX to establish foundational design parameters for optimal performance at various morphing configurations. CGull's wings were designed with two coupled morphing degrees-of-freedom (DOF) to allow the inner wing to bend forward and the feathered outer wing to retract backwards, mimicking the movement of the GBBG. The implementation of actuated morphing wings replaces the use of traditional ailerons for maneuverability and roll control. A compact actuation mechanism was developed to control three DOFs in the tail: pitching, tilting, and feather expansion. The tail's functionality provides added pitch control without elevators, and slight yaw control. Laminated composite structures were utilized in various components, such as the feathers and the skin of the fuselage and wings. A proof-of-concept prototype was built, and actuation tests were performed to prove the effectiveness of the proposed design and selected actuators. CGull's morphing design can effectively replicate the GBBG's non-flapping flight, optimizing the UAV's performance compared to its traditional fixed-wing UAV counterpart.

I. Introduction

A lot of morphing wing designs proposed in the literature enabled unmanned aerial vehicles (UAVs) to have wing deformations that resemble avian wing deformations [1,2]. Examples include span-morphing [3,4], twist-morphing [5–7], and camber-morphing [8–10] wing designs. However, most of these designs focused on only one degree of freedom, unlike birds that have different degrees of freedom in their wings giving them advanced capabilities to change the shape of their wings. In addition, most of these designs also lacked important features in avian wings, such as the location of the joints, the presence of feathers, and the spanwise variation of the wing profile. Accordingly, the performance of such wing designs could not match the efficient performance of avian wings. Moreover, only a few of the proposed wing designs were assembled to a fuselage or designed as a subsystem of a full UAV. Examples of morphing UAV designs include the Transformer aircraft [3], MataMorph-2 [6] and MataMorph-3 [10]. Not all of these morphing UAV designs featured morphing tails or had bio-inspired fuselage or tail designs. Morphing wings were retrofitted to a traditional fuselage design in many reported UAV designs, with possibly a traditional tail design [3].

Birds hold a distinct advantage over fixed wing aircraft especially when it comes to agility and adaptability [11]. However, creating UAV designs that mimic all biological features of birds, such as bones, joints, muscles, skin, and

[1] Undergraduate Student, Mechanical Engineering, AIAA Student Member.
[2] Associate Professor, Mechanical Engineering, AIAA Professional Member.

feathers remain an engineering challenge from the structural and control points of view. Bio-inspired flapping and non-flapping UAVs have been reported mainly in the last decade [12–14], with the recent advances in composite and lightweight materials, 3D-printing, and mini-servomotor technology. Non-flapping designs are more energy efficient and less complicated than flapping designs [15]. Focusing on non-flapping designs, UAVs were designed based on different species [16]. For example, the design of "Lishawk" [17] was inspired by the flight of the Northern Goshawk, and featured five-degrees of freedom, namely independent left and right wing feather expansion, tail pitch, tail yaw, and tail feather expansion. "LisEagle" [18] was inspired by the flight of eagles, and introduced wing pitching deformation to further improve the turning performance. "PigeonBot" [19] got inspiration from the pigeon, and used real biological feathers in its sweep-morphing wings. Tail pitch, tilt, and asymmetric feather expansion were proposed in [20]. Outer wing feather spread was developed and tested in [21]. Wing dihedral-morphing and tail tilting designs were also proposed [22] using flexible 3D-printed materials. The function of the tail in these UAVs is equally important as the wing because they play a big role in the stability and control of the UAV. For instance, wind tunnel tests performed on the tail mechanism developed by Murayama *et al.* [20] showed that changing the tilt angle, while having a downward elevation, generates lateral forces in the yaw direction. Controlling tail tilt allowed for more control over yaw without affecting efficiency.

Harvey and Inman [23] presented a literature review on methods used to quantify the aerodynamic efficiency of gliding birds and compared them to comparable UAVs. Their survey highlighted the high efficiency of gliding birds in subcritical Reynold's number (Re) regimes, suggesting that future avian-inspired morphing UAVs can extend their operational capabilities into lower Re ranges. The recent review on avian-inspired morphing for UAV flight control by Harvey *et al.* [16] highlighted the effects of wing sweep-, dihedral-, twist-, and camber-morphing, as well as tail incidence, spread, and rotation on the longitudinal and lateral control of UAVs. The review also surveyed coupled wing-tail morphing designs, as an emerging area of study. Focusing on the flight and inertial characteristics of 22 bird species, Harvey *et al.* [24] showed that birds can transition between stable and unstable states via wing morphing. They found that wing morphing allows birds to substantially change their roll and yaw inertia but has a minimal effect on the position of the center of gravity.

This paper presents a UAV design, named "CGull," which resembles the shape, size, and gliding flight of the Great Black Backed Gull (GBBG), *Larus marinus*. CGull features two coupled degrees of freedom in the wing to sweep the middle wing forward and the feathered outer wing backward, while retracting the wing feathers. CGull's tail has three degrees of freedom to pitch, tilt, and sweep the tail feathers. The wing features a fixed 7-degree dihedral angle and a 3.5-degree angle of incidence to represent the seagull's wing characteristics more accurately. Carbon fiber composites were used in manufacturing various structural components in CGull, such as the fuselage, wing covers, and feathers, to increase the specific stiffness and strength and to mimic the biological construction of the alternative bird organs that are naturally made of fibers. The rest of the paper is organized as follows: Section II presents a preliminary computational model developed in MachupX. Section III gives a detailed design description of all subsystems of CGull. Section IV details the manufacturing and testing of CGull. A final conclusion is given in Section V.

II. Preliminary Computational Model

The development of CGull initiated with the selection of a specific seagull species whose anatomical and flight performance characteristics could be mimicked to a close extent, given design and manufacturing constraints. The adult male Great Black Backed Gull (GBBG), weighing up to 2,275 grams, with a wingspan of 145 to 185 cm, and body length of 61 to 78 cm [25], was chosen as the inspiration for the target planform shape, wingspan, weight, and flight speed. Scans of seagull wings suggest that the high lift and low Reynolds number S1223-il airfoil closely resembles their span-averaged cross-sectional wing profile [26]. Since the exact species of seagull that these scans were obtained from was unspecified, it was assumed that the GBBG has a similar cross-sectional profile to the S1223-il airfoil for the purposes of creating a preliminary model. Admittedly, seagull wings cannot be accurately approximated by a singular, continuous airfoil but rather a distribution of different airfoils along the wingspan. Research focused on replicating the airfoil shapes along the wing of the common seagull have shown that the custom Liu S20 and Liu S40 as well as the NACA 3603 airfoils are suitable representations as well [26,27].

A numerical model of CGull was developed using MachUpX, an open-source python-based software developed by the Utah State University AeroLab [28]. MachUpX employs a numerical lifting-line algorithm with modifications based on the works of Reid and Hunsaker [29] and Goates and Hunsaker [30] to model the aerodynamic characteristics of any custom aircraft. MachUpX also has a complimentary python module for modeling airfoils, called AirfoilDatabase. In AirfoilDatabase, any airfoil coordinates data can be imported and then utilized in a python script to calculate airfoil properties. From these calculations either an airfoil database, a polynomial fit, or linear coefficients describing the characteristics of the airfoil can be generated. Subsequently, any of these files can then be imported

into MachUpX to describe the construction of an aircraft using the airfoil data in addition to other geometric parameters. A "scene," or the conditions the aircraft is placed in (i.e. density, kinematic viscosity, angle of attack, and velocity) should be defined. Finally, a python script computes the aerodynamic forces, moments, and coefficients of the aircraft based on the conditions described.

The preliminary model of CGull was defined in an aircraft object file in MachUpX, as a set of wings and a tail, as shown in Fig. 1(a). The reason for the exclusion of the fuselage was due to the limitations of the numerical lifting-line method MachUpX employs. This particular method is mainly intended to accurately predict the lift distribution of straight and swept wings of varying geometries [29,30]. The aircraft was defined in a three-dimensional space where the *x*-axis, *y*-axis, and *z*-axis correspond to the aircraft's longitudinal, lateral (i.e. along the wingspan), and vertical directions, respectively, as shown in Fig. 1. The wings of the preliminary model were defined in two spanwise segments of inner and outer wings for the left and right sides. The airfoil profile across the wings consisted of three linearly blended airfoils. Starting from the root chord, the inner wing segments are assigned the S1223-il airfoil profile. The outer wings start with S1223-il and gradually transform to the NACA 2410 airfoil profile along 50% of their span with the remainder gradually transforming into the NACA 0006 airfoil profile. A fixed 7-degree dihedral angle was assigned to the whole wing. The tail was defined as two spanwise segments mirrored on the left and right sides and the NACA 0006 profile was assigned across its entire span. The airfoils were defined by three files containing polynomial fits of each airfoil's characteristics which were generated using AirfoilDatabse.

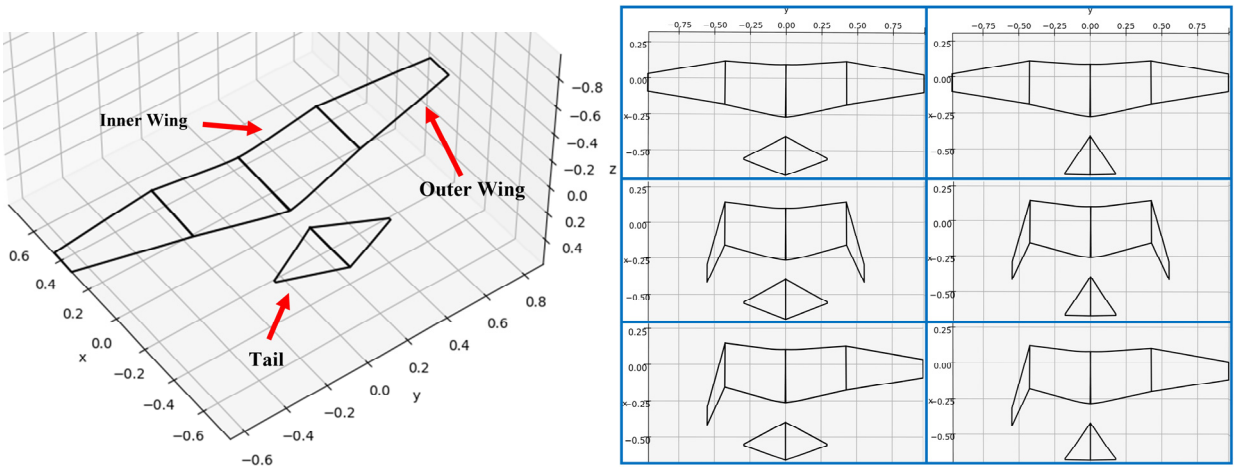

(a) **(b)**

Fig. 1 (a) CGull's preliminary computational model in MachUpX, (b) Six considered morphing wing and tail configurations.

The NACA 2410 and NACA 0006 airfoils were selected with the eventual manufacturing process in mind. To be specific, the fully realized design of CGull was set to have artificial wing and tail feathers. The NACA 0006 was selected to represent those feathers which would be manufactured from composite materials and have a flat uncambered geometry. The NACA 0006 is a suitable representation of these artificial feathers for its thin and symmetrical profile. The NACA 0006 also offered a continuous rounded leading edge for the wings and tail similar to the leading-edge sections to be used in the physical model. NACA 2410 airfoil was also used to represent a cover surface that would be fitted over a portion of the feathers along the wingspan of the physical model. This cover was anticipated to reduce drag at the leading edge and create a smooth transition from the inner wings designed with the S1223-il airfoil and the outer wings made up of flat feathers. The center of gravity (C.G.) of the preliminary model was not changed from the default settings predefined by MachUpX. As such the C.G. remained fixed to the origin of the body-fixed coordinate system which corresponds to a quarter of the chord of the aircraft's main wings.

The geometries of the wings and tail of the preliminary model were manipulated to initially produce six different configurations for a handful of wing and tail morphing combinations. These configurations, shown in Fig. 1(b), include (a) fully extended wings with a fully extended tail, (b) fully extended wings with a tucked tail, (c) tucked wings with an extended tail, (d) tucked wings with a tucked tail, (e) asymmetric wings with an extended tail, and (f) asymmetric wings with a tucked tail. For the fully extended wing configurations, the inner and outer wings totaled a combined wingspan of 185 cm with a planform area of 4,756 cm^2. The wingspan was reduced by approximately 57% of the extended wingspan to 106 cm for the tucked wing configuration. The wing area decreased by about 66% to 3,116 cm^2 from the extended wing to the tucked wing configuration. The asymmetric wing configurations were created by

combining the left inner and outer wing segments of the tucked wing configuration with the right inner and outer wing segments of the extended wing configuration. As such, the wingspan and area of this configuration were 146 cm and 3,936 cm^2, respectively. The extended tail had a span of 56 cm and a planform area of 756 cm^2 which were reduced to a span of 34 cm and an area of 459 cm^2 for the tucked tail. For all configurations, each wing segment was given a grid size of 90 horseshoe vortices to be modeled in the numerical lifting-line algorithm MachUpX employs. This number of vortices was found to provide a sufficient distribution of control points along the wing and tail segments as it achieved convergence of the nonlinear solver within a manageable number of iterations at the default convergence threshold. MachUpX's nonlinear solver was employed with a convergence tolerance of 10^{-10} and a relaxation factor of 1.0 for the calculation of the aerodynamic forces and moments of each configuration. The estimated UAV weight was assigned to be 2 kg (19.62 N).

Standard atmospheric, sea-level flight conditions were defined in the scene object file for all of the six wing and tail morphing configurations. A density of 1.23 kg/m^3 and a kinematic viscosity of 1.46×10^{-5} m^2/s were inputted as parameters defining the scene. The velocity of the aircraft was set to 13.4 m/s (approximately 30 mph) which is typically the highest flight speed that seagulls can reach [31]. The lift and drag forces as well as the roll, pitch, and yaw moments acting on the aircraft were recorded for an angle of attack (AOA) range of -5° to 16°. The force and moment quantities obtained were non-dimensionalized using the following equations.

$$C_L = \frac{2F_L}{\rho V^2 S}; \quad C_D = \frac{2F_D}{\rho V^2 S}; \quad C_l = \frac{2M_x}{\rho V^2 Sb}; \quad C_m = \frac{2M_y}{\rho V^2 Sc}; \quad C_n = \frac{2M_z}{\rho V^2 Sb} \tag{1}$$

where C_L and C_D are the lift and drag coefficients, respectively, C_l , C_m , and C_n are the roll, pitching, and yaw moment coefficients, respectively. F_L and F_D are the lift and drag forces, respectively, M_x is the roll moment about the x-axis, M_y is the pitching moment about the y-axis, and M_z is the yaw moment about the z-axis. Lastly, ρ is the density of air, V is the aircraft velocity, S is the planform area of the main wings, b is the wingspan, and c is the mean wing chord.

Fig. 2(a and b) show the lift and drag forces, respectively, versus AOA for the four symmetric wing and tail morphing configurations, while Fig. 2(c) shows the aerodynamic efficiency (L/D). It can be seen that wing extension increases both the lift and drag forces, as it increases the wing area. The generated lift can balance the estimated UAV weight at 0° AOA when the wings are extended, and at 4° AOA when the wings are tucked. Tail expansion has little effect on both forces, given the relatively smaller change in area of the tail compared to that of the wings. The maximum aerodynamic efficiency is achieved at an AOA of 5°. Extending the wings can significantly change the generated aerodynamic lift and efficiency. The results are in general agreement with the findings of Ajanic *et al.* [17] from wind tunnel tests on LisHawk, which is a smaller bird-like UAV.

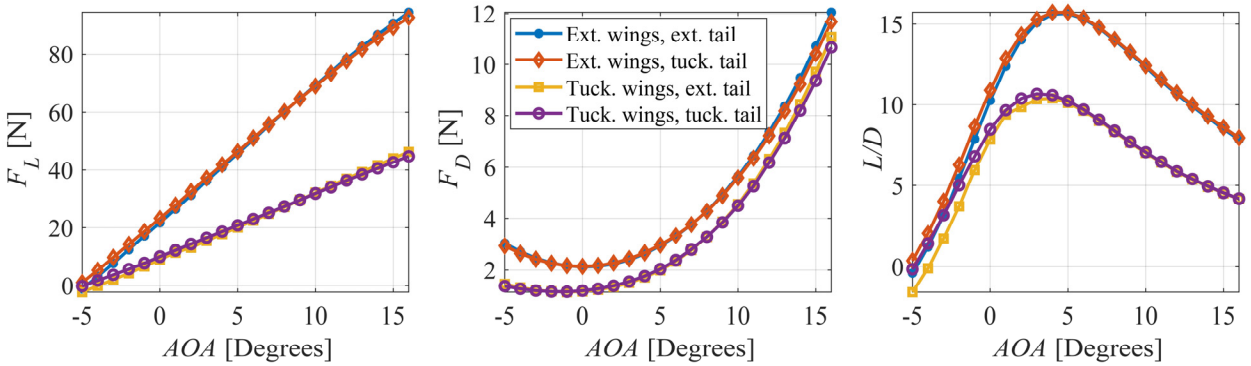

(a) **(b)** **(c)**

Fig. 2 (a) Lift force, (b) Drag force, and (c) L/D vs AOA for four different configurations

The effect of tail pitching is presented in Fig. 3. It can be seen from Fig. 3a that the lift coefficient can be increased or decreased by pitching the tail down or up, respectively. This is also in agreement with the results of Ajanic *et al.* [17]. The pitching moment coefficient is significantly affected by pitch morphing, as shown in Fig. 3b. The slope of the curve is negative for all cases up to a specific AOA, indicating a stable flight. At high AOAs, the slope becomes positive, rendering the UAV unstable. This instability happens earlier when the tail is pitched down.

The effect of tail tilt on the yaw and roll moments is presented in Fig. 4(a and b). Since the values of the roll moment coefficient are relatively small for tail tilt angles up to 30°, tail tilt can be used for fine tuning of the roll motion. The effect of asymmetric wing morphing on roll moment coefficient is included in Fig. 4(c) to show how this morphing actuation is much more significant on the generated roll moment compared to tail tilting.

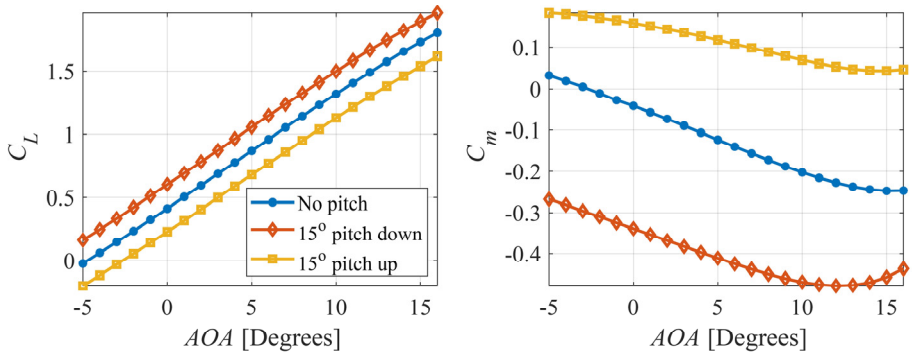

(a) **(b)**

Fig. 3 Effect of tail pitch on (a) lift coefficient, (b) pitching moment coefficient

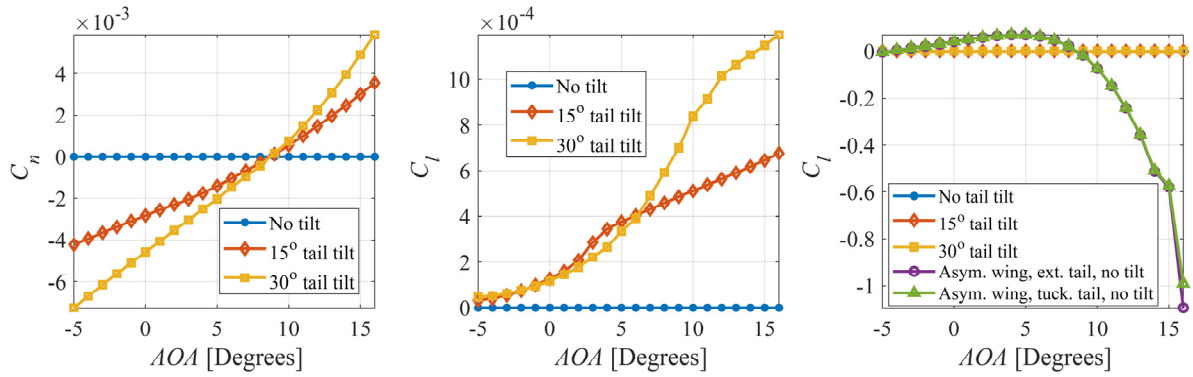

(a) **(b)** **(c)**

Fig. 4 Effect of tail tilt on (a) yaw moment coefficient, and (b) roll moment coefficient, (c) Effect of asymmetric wing morphing on roll moment coefficient.

III. Model Description

A. Overall Design

Fig. 5 shows the full CAD model of CGull. The inner wings are integrated to the fuselage making one sturdy composite structure. Servomotors in the fuselage actuate both the inner and outer wings in a coupled motion through a linkage mechanism, enabling each wing to sweep back individually. The fuselage includes a rear bracket for the tail structure and a front support for the motor. The tail includes two servomotors for pitch and tilt morphing, in addition to a linear actuator for the feather expansion mechanism. The dimensions follow those of the MachUpX model.

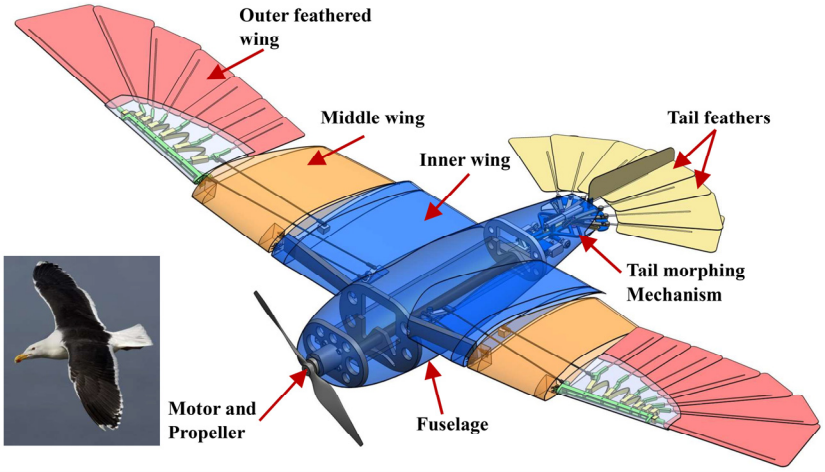

Fig. 5 Full CAD model of CGull

Although the preliminary computational model showed that tail tilt and feather expansion have minimal effects on the generated roll moment and lift force, respectively, these two tail morphing degrees of freedom were kept to experimentally investigate their effects, given that real birds have this ability and are using them in various maneuvers.

B. Wing design

The wings of CGull achieve morphing with two coupled degrees of freedom which mimic the movement of the elbow and wrist of the gull. This effectively divides the wing into three sections: a rigidly attached inner wing, a forward sweeping midwing and an aft sweeping segmented feather outer wing, as shown in Fig. 6a. While the feathered portion of the wing provides the area change needed for lift and drag reduction and roll control, the forward sweeping midwing maintains some level of maneuverability as the outer wing pushes the center of pressure rearward. A 7-degree fixed dihedral was added to aid in yaw stability and a 3.5-degree angle of incidence at the root which washes out to 0-degree at the tip provides maximum lift at low speeds while providing stability during stall onset.

A single 6kg-cm servomotor for each wing acts on both degrees of freedom and is located in the wing root area (Fig. 6a). Carbon fiber rods of 2mm diameter are used as linkages with ball joint ends to allow articulation. Feather retraction is achieved by holding the innermost feather fixed to the inner wing by the feather actuation link and the outermost feather in line with the outer wing structure (Fig. 6a). As the outer wing structure is swept back, a 3D-printed Thermoplastic polyurethane (TPU) spring keeps the feathers evenly spaced while allowing for the relative motion to overlap the feathers. To reduce weight and complexity, the number of feathers was reduced to seven larger prepreg carbon fiber plates instead of the gulls ten primary feathers. Carbon fiber is used extensively in the wing design of CGull. Due to its strength and stiffness, carbon fiber skin sections are used as load-carrying members to carry the loads between the joints. Hinge sections are 3D-printed from PLA which conform to the leading edge of the wings and allow for large bonding areas. The outer wing structure and feather holders are also 3D-printed from PLA.

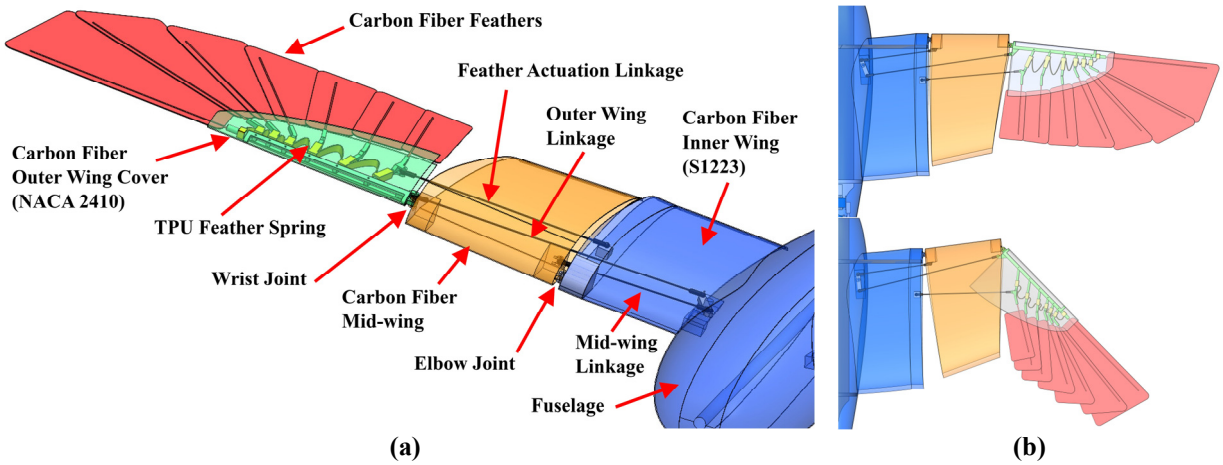

Fig. 6 (a) CGull's wing design, (b) Wing in expanded and tucked configurations

C. Tail Design

CGull's morphing tail implements three degrees of freedom to perform its morphing motions of feather expansion, pitching and tilting, as shown in Fig. 7a. Expansion of the feathers, essential to an increase in the lift force due to greater surface area, is performed via a slider mechanism. The feather shafts are carbon fiber rods of 2 mm diameter that are sandwiched between two carbon fiber plies that make up the feather vane. One ply takes the outer profile of the feather while the other is placed around the central area to bond the shaft to the vane. The feather shafts are inserted in the holes of the feather spokes. Feather expansion/contraction happens when the linear actuator pushes the slider, which moves the two pins along the slots in the slider and base plate. The motion of the pins rotates the spokes, resulting in feather expansion or contraction.

The whole mechanism is mounted on the base plate which is 3D-printed of PLA but has a 2-ply carbon fiber laminate on the bottom for reinforcement. To perform the seagull's tail pitching and tilting mimicry, a system of two servomotors, independently actuated, facing opposite directions, was developed. With this setup, the two servomotor arms rotating symmetrically perform the equivalent of the tail pitching, whereas the arms revolving asymmetrically result in tail tilting clockwise or counterclockwise, depending on which servomotor arm is actuated up or down. The system includes two housings for the servomotors on a bracket and rotational ball joints. The maximum and minimum planner feather expansion angles are 130° and 47°, as shown in Fig. 7b. HiTec HS-645MG High Torque Servos (9.6

kg/0.2s) were used, along with the USLICCX electric micro linear actuator (12 V – 1.2 “ stroke, 64 N, speed 0.6 inch/s).

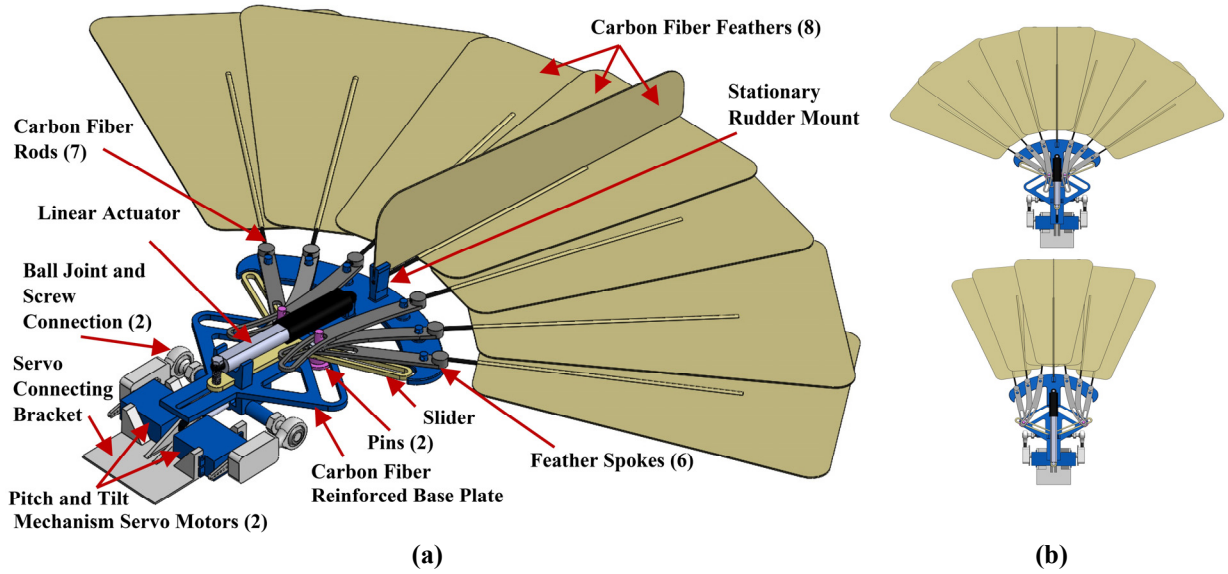

Fig. 7 (a) CGull’s tail design, (b) Tail in expanded and contracted configurations

D. Fuselage Design

CGull’s fuselage is based on a NACA 0020 symmetric airfoil profile which closely mimics the shape of the common seagull’s body [27]. The profile was widened to make more room for avionics, and the inner wings were merged into the fuselage to form a single structure, as shown in Fig. 8a. Although the fuselage and inner wing skins are intended to carry the applied aerodynamic loads, a central 25mm carbon-fiber tube was added longitudinally for additional strength. This tube is attached to the fuselage through two rings cut from a carbon/Nomex sandwich panel, as shown in Fig. 8a. Access to the fuselage's interior is through a removable nose cone which slides out from the front with the attached avionics tray, as shown in Fig. 8b. Access to the tail morphing mechanism is through a rear hatch, also shown in Fig. 8b.

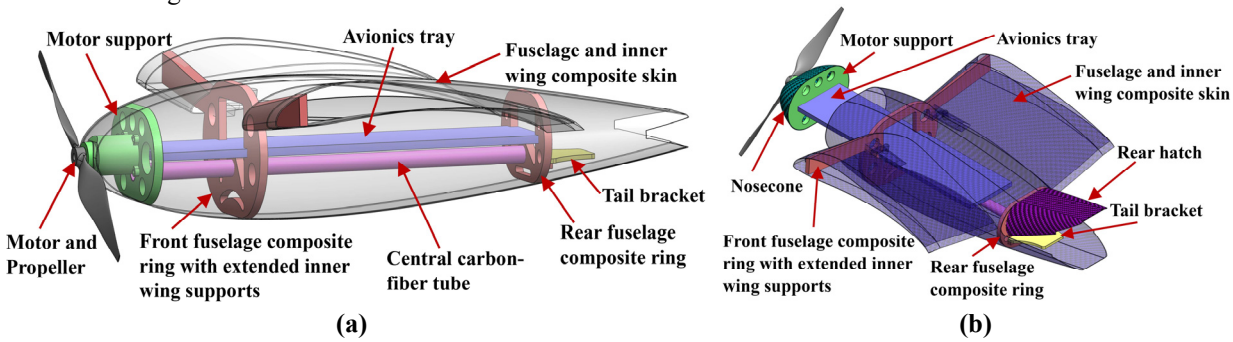

Fig. 8 (a) CGull’s fuselage structure (b) fuselage and inner wing composite skin and fuselage access points

E. Propulsion and Avionics System

As CGull is a non-flapping design, a Spektrum 4240 brushless DC motor and a 12 × 6” 2-vane nylon propeller are used to generate thrust. Electrical power is supplied by a 18.5V LiPo battery to the Spektrum 45A ESC which controls the motor and outputs a regulated 7.2V source for the avionics (Fig. 9). The avionics system consists of a FRSKY XR8 receiver and an Arduino Nano RP2040 Connect which runs a custom MicroPython script. The XR8 receives radio signals from the ground controller and sends them over SBUS to the Arduino through an inverter circuit. PWM signals are then generated by the Arduino and sent to the servo motors corresponding to the commands received.

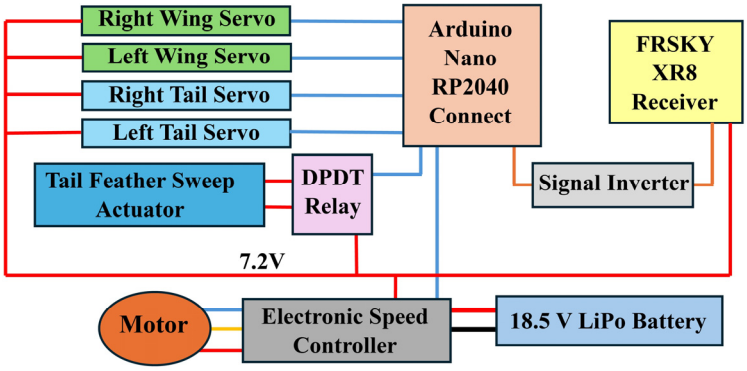

Fig. 9 CGull's avionics diagram

IV. Manufacturing and Testing

The wet layup composite manufacturing technique was selected for building the fuselage and inner wing skin due to the highly curved surface of this structure and the flexibility of this manufacturing technique. Upper and lower female molds were first constructed individually. Each mold was divided into multiple parts that can be 3D printed individually, and then assembled using bolts. An exploded and assembled views of the lower skin mold are shown Fig. 10a. This approach has two benefits. First, the parts can be disconnected by the end of the cure process to facilitate the release process. Second, any of the parts can be replaced in case it gets damaged from repeated use. A high-density foam, commonly used for composite molds, would lack these two benefits, and the negative draft angle at the nose would have been impossible to achieve with a traditional CNC router. To improve surface finish and ease part release, the molds were smoothed with multiple steps of automotive body filler and sanded with a final coating of Duratec polyester surface primer. The final mold preparation consisted of wet sanding of 2500 grit and 6 coats of mold release wax. Fig. 11 shows the assembled and finalized lower mold, and the upper mold prior to the final sanding step. Two plies of carbon-fiber weave were used for constructing the skin in the wet-layup process.

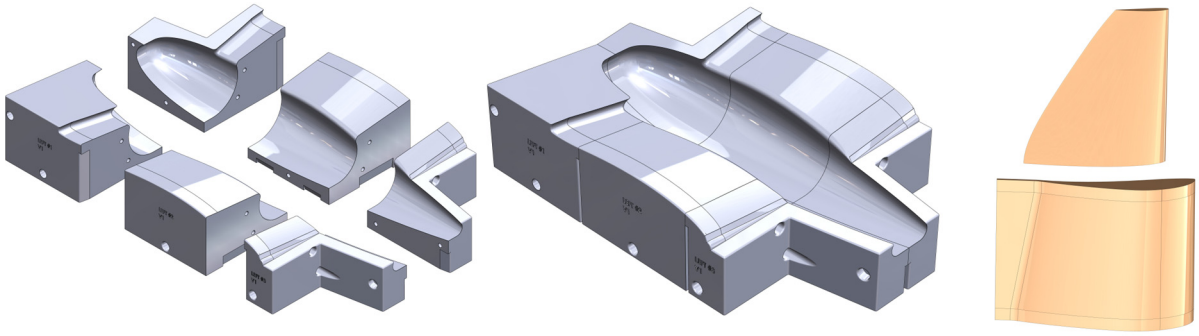

(a) **(b)**

Fig. 10 (a) Exploded and assembled views of the fuselage and inner wing lower mold, (b) Middle and outer wing skin molds

Male molds were designed and 3D-printed for the middle and outer wing composite skin, as shown in Fig. 10b. The middle wing skin mold had an extended trailing edge to separate the upper and lower surfaces during manufacturing for easier mold release. The molds were sanded to obtain a smooth surface finish, and then were totally covered by a release film. Two plies of woven carbon fiber were used in the wet-layup process. Post-processing, after curing and mold release, trimmed all edges, bringing each skin section to its desired size, and bonded the upper and lower surfaces at the trailing edge. Fig. 11 also shows these molds with the middle and outer skin placed on them for demonstration.

Feathers were manufactured from two plies of CYCOM 5350 woven carbon fiber prepreg sandwiching 2 mm dia. carbon fiber rods that act as feather shafts. To reduce weight, the top layer has a smaller surface area than the bottom one, and the shafts are not extended all the way to the feather tip, as shown in Fig. 12a. This construction reinforced the central area of the feathers around the shafts. A flat tempered glass plate was used as mold. The vendor-recommended cure cycle was followed in an autoclave. All manufactured composite structures are demonstrated in Fig. 12b. The fuselage rings and the avionics tray were cut from a sandwich composite panel that has two plies in each

face plate and a honeycomb 5 mm thick Nomex core. The tail base plate was printed with carbon-fiber reinforced PLA, and a 2-ply carbon-fiber laminate was bonded to it bottom to further reinforce it. All other components were 3D-printed and assembled. The wing and tail servomotors and the tail linear actuator were also assembled. The total weight of the tail subassembly is 371 g, and the fuselage with wings and avionics altogether weight 1,158 g. The total weight is 1,529 g, which is around 25% less than the estimated weight used in the preliminary calculations stage.

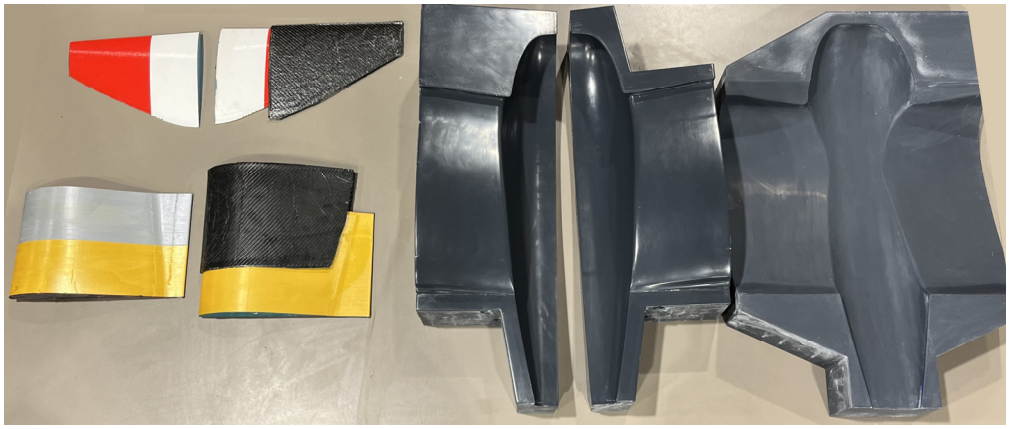

Fig. 11 3D-printed molds used for composite manufacturing

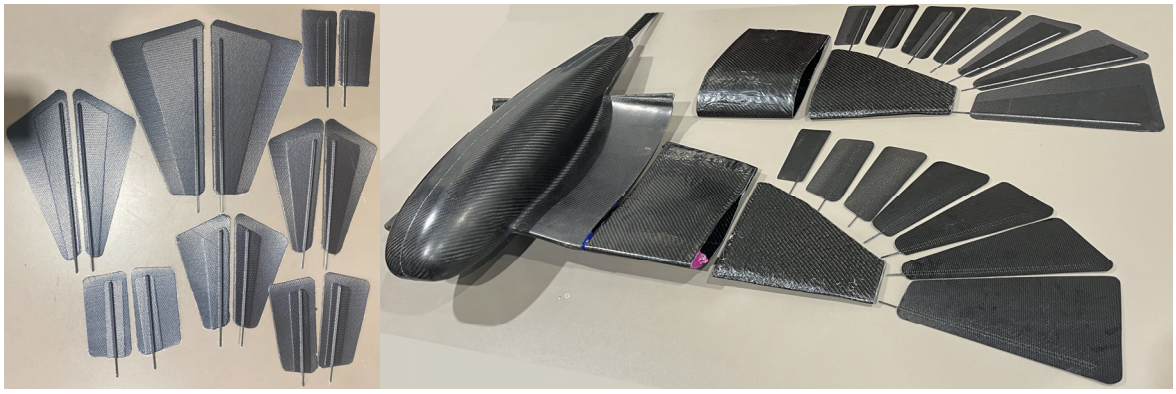

(a) **(b)**

Fig. 12 (a) Wing composite feathers, (b) Composite structures: Fuselage and inner wing, middle wings, outer wings with feathers.

Wing actuation test is shown in Fig. 13, while tail feather expansion actuation is shown in Fig. 14. All actuators are motors proved to be capable of actuating the morphing structures efficiently. A bottom view of CGull's prototype assembly is shown in Fig. 15.

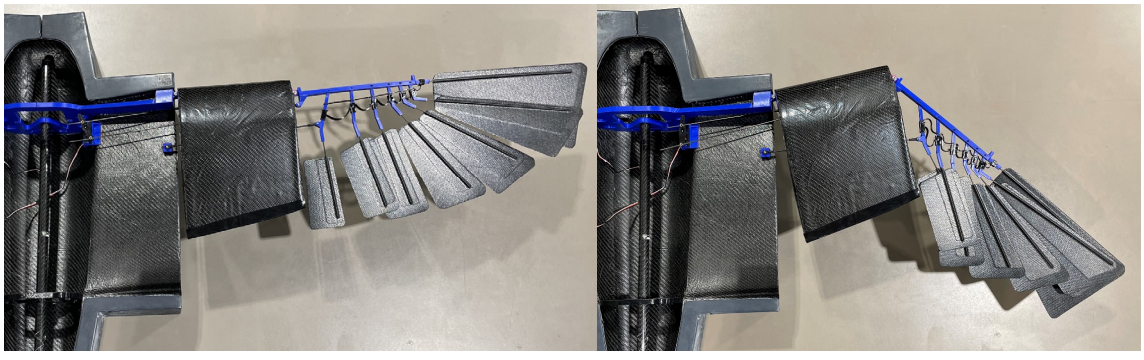

Fig. 13 Wing actuation; Fuselage and inner wing lower skin is placed on its mold, upper skin is removed for demonstration, outer wing composite skin is also removed to show the feather expansion mechanism.

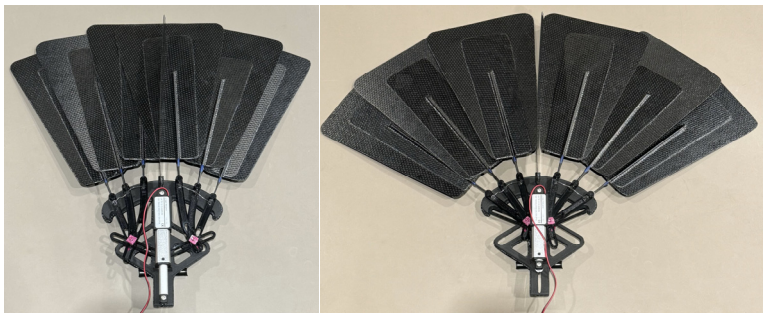

Fig. 14 Tail feather expansion actuation

Fig. 15 Bottom view of CGull's prototype

V. Summary and Conclusion

This paper presents the design of CGull, a bio-inspired non-flapping UAV, that features a significant number of composite structures. A numerical model created in MachUpX was first developed to understand the effects of the various morphing degrees of freedom on the generated aerodynamic forces and moments. Prototypes of all subsystems were manufactured and assembled. Actuation tests validated the design choices, and qualified CGull's prototype for flight tests to follow.

Acknowledgments

This work was done by the eighth cohort of the "Smart Morphing Wing" research-based senior design project at California State University, Northridge (CSUN). The authors acknowledge the support of the following members: Peter Niednagel, Eric Bertuch, Ivan Rodriguez, Trent Bird, Behafarin Sharifi, Sebastian Campos, Paola Ramos, Brian Sanchez, Matthew Brody, and Gerbert Funes Alfaro. The authors acknowledge the Mechanical Engineering Department, the Instructionally Related Activities (IRA) grant, and the Student Travel and Academic Research (STAR) program at CSUN.

References

[1] Barbarino, S., Bilgen, O., Ajaj, R. M., Friswell, M. I., and Inman, D. J., "A Review of Morphing Aircraft," *Journal of Intelligent Material Systems and Structures*, Vol. 22, No. 9, 2011, pp. 823–877. https://doi.org/10.1177/1045389X11414084

[2] Sun, J., Guan, Q., Liu, Y., and Leng, J., "Morphing Aircraft Based on Smart Materials and Structures: A State-of-the-Art Review," *Journal of Intelligent Material Systems and Structures*, Vol. 27, No. 17, 2016, pp. 2289–2312. https://doi.org/10.1177/1045389X16629569

[3] Ajaj, R. M., and Jankee, G. K., "The Transformer Aircraft: A Multimission Unmanned Aerial Vehicle Capable of Symmetric and Asymmetric Span Morphing," *Aerospace Science and Technology*, Vol. 76, 2018, pp. 512–522. https://doi.org/10.1016/j.ast.2018.02.022

[4] Bishay, P. L., Burg, E., Akinwunmi, A., Phan, R., and Sepulveda, K., "Development of a New Span-Morphing Wing Core Design," *Designs*, Vol. 3, No. 1, 2019, p. 12. https://doi.org/10.3390/designs3010012

[5] Rodrigue, H., Cho, S., Han, M.-W., Bhandari, B., Shim, J.-E., and Ahn, S.-H., "Effect of Twist Morphing Wing Segment on Aerodynamic Performance of UAV," *Journal of Mechanical Science and Technology*, Vol. 30, No. 1, 2016, pp. 229–236. https://doi.org/10.1007/s12206-015-1226-3

[6] Schlup, A., Bishay, P., Mclennan, T., Barajas, C., Talebian, B., Thatcher, G., Flores, R., Perez-Norwood, J., Torres, C., Kibret, K., and Guzman, E., "MataMorph 2: A New Experimental UAV with Twist-Morphing Wings and Camber-Morphing

Tail Stabilizers," presented at the AIAA Scitech 2021 Forum, VIRTUAL EVENT, 2021. https://doi.org/10.2514/6.2021-0584
[7] Bishay, P. L., and Aguilar, C., "Parametric Study of a Composite Skin for a Twist-Morphing Wing," *Aerospace*, Vol. 8, No. 9, 2021, p. 259. https://doi.org/10.3390/aerospace8090259
[8] Fincham, J. H. S., and Friswell, M. I., "Aerodynamic Optimisation of a Camber Morphing Aerofoil," *Aerospace Science and Technology*, Vol. 43, 2015, pp. 245–255. https://doi.org/10.1016/j.ast.2015.02.023
[9] Bishay, P. L., Finden, R., Recinos, S., Alas, C., Lopez, E., Aslanpour, D., Flores, D., and Gonzalez, E., "Development of an SMA-Based Camber Morphing UAV Tail Core Design," *Smart Materials and Structures*, Vol. 28, No. 7, 2019, p. 075024. https://doi.org/10.1088/1361-665X/ab1143
[10] Bishay, P. L., Kok, J. S., Ferrusquilla, L. J., Espinoza, B. M., Heness, A., Buendia, A., Zadoorian, S., Lacson, P., Ortiz, J. D., Basilio, R., and Olvera, D., "Design and Analysis of MataMorph-3: A Fully Morphing UAV with Camber-Morphing Wings and Tail Stabilizers," *Aerospace*, Vol. 9, No. 7, 2022, p. 382. https://doi.org/10.3390/aerospace9070382
[11] Brown, R. H. J., "THE FLIGHT OF BIRDS," *Biological Reviews*, Vol. 38, No. 4, 1963, pp. 460–489. https://doi.org/10.1111/j.1469-185X.1963.tb00790.x
[12] Basri, E. I., Basri, A. A., and Ahmad, K. A., "Computational Fluid Dynamics Analysis in Biomimetics Applications: A Review from Aerospace Engineering Perspective," *Biomimetics*, Vol. 8, No. 3, 2023, p. 319. https://doi.org/10.3390/biomimetics8030319
[13] Budholiya, S., Bhat, A., Raj, S. A., Hameed Sultan, M. T., Md Shah, A. U., and A. Basri, A., "State of the Art Review about Bio-Inspired Design and Applications: An Aerospace Perspective," *Applied Sciences*, Vol. 11, No. 11, 2021, p. 5054. https://doi.org/10.3390/app11115054
[14] Han, J., Hui, Z., Tian, F., and Chen, G., "Review on Bio-Inspired Flight Systems and Bionic Aerodynamics," *Chinese Journal of Aeronautics*, Vol. 34, No. 7, 2021, pp. 170–186. https://doi.org/10.1016/j.cja.2020.03.036
[15] Mackenzie, D., "A Flapping of Wings," *Science*, Vol. 335, No. 6075, 2012, pp. 1430–1433. https://doi.org/10.1126/science.335.6075.1430
[16] Harvey, C., Gamble, L. L., Bolander, C. R., Hunsaker, D. F., Joo, J. J., and Inman, D. J., "A Review of Avian-Inspired Morphing for UAV Flight Control," *Progress in Aerospace Sciences*, Vol. 132, 2022, p. 100825. https://doi.org/10.1016/j.paerosci.2022.100825
[17] Ajanic, E., Feroskhan, M., Mintchev, S., Noca, F., and Floreano, D., "Bioinspired Wing and Tail Morphing Extends Drone Flight Capabilities," *Science Robotics*, Vol. 5, No. 47, 2020, p. eabc2897. https://doi.org/10.1126/scirobotics.abc2897
[18] Ajanic, E., Feroskhan, M., Wüest, V., and Floreano, D., "Sharp Turning Maneuvers with Avian-Inspired Wing and Tail Morphing," *Communications Engineering*, Vol. 1, No. 1, 2022, p. 34. https://doi.org/10.1038/s44172-022-00035-2
[19] Chang, E., Matloff, L. Y., Stowers, A. K., and Lentink, D., "Soft Biohybrid Morphing Wings with Feathers Underactuated by Wrist and Finger Motion," *Science Robotics*, Vol. 5, No. 38, 2020, p. eaay1246. https://doi.org/10.1126/scirobotics.aay1246
[20] Murayama, Y., Nakata, T., and Liu, H., "Aerodynamic Performance of a Bird-Inspired Morphing Tail," *Journal of Biomechanical Science and Engineering*, Vol. 18, No. 1, 2023, pp. 22-00340-22–00340. https://doi.org/10.1299/jbse.22-00340
[21] Di Luca, M., Mintchev, S., Heitz, G., Noca, F., and Floreano, D., "Bioinspired Morphing Wings for Extended Flight Envelope and Roll Control of Small Drones," *Interface Focus*, Vol. 7, No. 1, 2017, p. 20160092. https://doi.org/10.1098/rsfs.2016.0092
[22] Bishay, P. L., Brody, M., Podell, D., Corte Garcia, F., Munoz, E., Minassian, E., and Bradley, K., "3D-Printed Bio-Inspired Mechanisms for Bird-like Morphing Drones," *Applied Sciences*, Vol. 13, No. 21, 2023, p. 11814. https://doi.org/10.3390/app132111814
[23] Harvey, C., and Inman, D. J., "Aerodynamic Efficiency of Gliding Birds vs Comparable UAVs: A Review," *Bioinspiration & Biomimetics*, Vol. 16, No. 3, 2021, p. 031001. https://doi.org/10.1088/1748-3190/abc86a
[24] Harvey, C., Baliga, V. B., Wong, J. C. M., Altshuler, D. L., and Inman, D. J., "Birds Can Transition between Stable and Unstable States via Wing Morphing," *Nature*, Vol. 603, No. 7902, 2022, pp. 648–653. https://doi.org/10.1038/s41586-022-04477-8
[25] Malling Olsen, K., and Larsson, H., "Gulls of Europe, Asia and North America," A & C Black, London, 2010.
[26] Liu, T., Kuykendoll, K., Rhew, R., and Jones, S., "Avian Wings," presented at the 24th AIAA Aerodynamic Measurement Technology and Ground Testing Conference, Portland, Oregon, 2004. https://doi.org/10.2514/6.2004-2186
[27] Harvey, C., Baliga, V. B., Goates, C. D., Hunsaker, D. F., and Inman, D. J., "Gull-Inspired Joint-Driven Wing Morphing Allows Adaptive Longitudinal Flight Control," *Journal of The Royal Society Interface*, Vol. 18, No. 179, 2021, p. 20210132. https://doi.org/10.1098/rsif.2021.0132
[28] "Machupx: Fast and Accurate Aerodynamic Modelling Using Lifting-Line Theory.," AeroLab, 2020.
[29] Reid, J. T., and Hunsaker, D. F., "A General Approach to Lifting-Line Theory, Applied to Wings with Sweep," presented at the AIAA Scitech 2020 Forum, Orlando, FL, 2020. https://doi.org/10.2514/6.2020-1287
[30] Goates, C. D., and Hunsaker, D. F., "Practical Implementation of a General Numerical Lifting-Line Method," presented at the AIAA Scitech 2021 Forum, VIRTUAL EVENT, 2021. https://doi.org/10.2514/6.2021-0118
[31] Shepard, E. L. C., Williamson, C., and Windsor, S. P., "Fine-Scale Flight Strategies of Gulls in Urban Airflows Indicate Risk and Reward in City Living," *Philosophical Transactions of the Royal Society B: Biological Sciences*, Vol. 371, No. 1704, 2016, p. 20150394. https://doi.org/10.1098/rstb.2015.0394